arXiv:1607.04300v1 [cond-mat.supr-con] 14 Jul 2016

Nodal-line pairing with 1D-3D coupled Fermi surfaces: a model motivated by Cr-based superconductors

Gideon Wachtel[1] and Yong Baek Kim[1, 2, 3]

[1] *Department of Physics, University of Toronto, Toronto, Ontario M5S 1A7, Canada*
[2] *Canadian Institute for Advanced Research/Quantum Materials Program, Toronto, Ontario MSG 1Z8, Canada*
[3] *School of Physics, Korea Institute for Advanced Study, Seoul 130-722, Korea*

Motivated by the recent discovery of a new family of Chromium based superconductors, we consider a two-band model, where a band of electrons dispersing only in one direction interacts with a band of electrons dispersing in all three directions. Strong $2k_f$ density fluctuations in the one-dimensional band induces attractive interactions between the three-dimensional electrons, which, in turn makes the system superconducting. Solving the associated Eliashberg equations, we obtain a gap function which is peaked at the "poles" of the three-dimensional Fermi sphere, and decreases towards the "equator". When strong enough local repulsion is included, the gap actually changes sign around the "equator" and nodal rings are formed. These nodal rings manifest themselves in several experimentally observable quantities, some of which resemble unconventional observations in the newly discovered superconductors which motivated this work.

I. INTRODUCTION

Recent experiments[1–3] have discovered superconductivity in a new family of Chromium based compounds, $K_2Cr_3As_3$, $Rb_2Cr_3As_3$, and $Cs_2Cr_3As_3$, which consist of well separated Cr_3As_3 chains. As sometimes expected for one-dimensional systems, enhanced heat capacity[1, 4] and unusual nuclear magnetic resonance (NMR) measurements[5] in the normal state indicate that electron-electron interactions play an important role. In the superconducting phase, experiments show signatures of an unconventional pairing mechanism, with nodes in the gap function. Among these are the absence of a Hebel-Slichter peak in NMR measurements[5], the linear decrease of the superfluid stiffness as seen in muon spin relaxation (μSR)[6] and penetration depth[7] experiments, and $\sqrt{H}$ increase in the specific heat[2] under an applied magnetic field H.

The electronic band structures of $K_2Cr_3As_3$ and $Rb_2Cr_3As_3$ have been calculated[8, 9], using Density Functional Theory (DFT), which finds a single three-dimensional (3D) Fermi-surface, and several quasi-one-dimensional (Q1D) Fermi surfaces, with electronic dispersion primarily along the Cr_3As_3 chains. Some of the Q1D Fermi surfaces nearly touch the 3D Fermi surface. We emphasize here the uniqueness of this band structure, as compared with other quasi-one-dimensional superconductors. While the electronic band structure is highly anisotropic in other Q1D superconductors[10, 11], in the Chromium based superconductors, anisotropic Q1D bands coexist, and interact, with a conventional, 3D band. Motivated by this observation, we ask, what kind of superconductivity can arise from coupling between electrons in Q1D and 3D bands.

To answer this question, we introduce a simplified model, consisting of a single one-dimensional (1D) band, with dispersion in only one direction, and a 3D band which disperses isotropically in all directions. The 1D Fermi-surface sheets touch the Fermi sphere at its "north and south poles", as depicted in figure 1a. One-dimensional electronic systems exhibit enhanced density fluctuations with a wave vector $2k_f$ where k_f is the Fermi momentum. A $2k_f$ wave vector also connects the two "poles" of the 3D Fermi sphere, allowing the 1D fluctuations to induce a strong attractive force between the opposite points. This effective attractive interaction is strongly dependent on momentum and energy, and can therefore give rise to pairing gap functions of an anisotropic d_{z^2}-wave nature, in addition to the more conventional uniform s-wave gap functions. Higher order functional forms are possible as well. When the local repulsion within the 3D band is strong enough to suppress s-wave superconductivity, a d_{z^2}-wave like gap function is expected to describe the leading supercoducting instability of the model. We show that indeed this is the case by numerically solving the Eliashberg equations for the effective interaction.

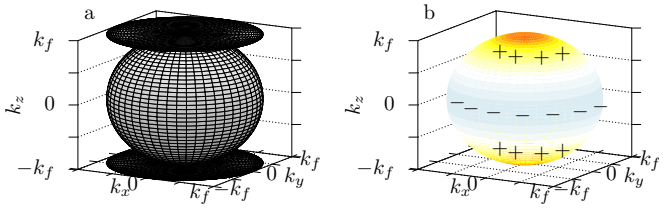

FIG. 1. Left: Fermi Surface geometry of the model, Eq. (1). The 1D Fermi sheets touch the 3D Fermi sphere at its "north and south poles". A $2k_f$ momentum transfer between the two 1D band sheets, is also an allowed momentum transfer between these points. Right: Gap function with nodal rings, plotted on the 3D Fermi shpere. Yellow-red regions indicate $\Delta(z) > 0$, while blue indicates $\Delta(z) < 0$. The gap nodes are depicted by the two white rings around the Fermi surface in the upper and lower hemispheres.

A gap function of a d_{z^2}-wave functional form is characterized by a change in sign as one moves away from the "poles" on the Fermi sphere, towards the "equator", see figure 1b. The points where the gap changes sign

form two gapless nodal rings in the upper and lower Fermi hemispheres. The presence of such nodes in the gap function, can manifest itself in various experimental signatures. We use the gap functions we obtained from solving the Eliashberg equations to show that our model is indeed expected to show unconventional behavior in NMR and superfluid stiffness measurements, similar to those observed in the Chromium based superconductors. Since our results rely on generic density-density interactions, the d_{z^2}-wave nodal ring pairing would be a viable candidate for the newly discovered superconducting phase in these materials.

II. 1D-3D COUPLED FERMI SURFACES

Consider a three-dimensional system with a band of spin half fermions (denoted by χ) dispersing only in one direction (k_z) and an additional band of spin half fermions (ψ) dispersing isotropically in all directions. The zero temperature imaginary time action of such a system is given by

$$S_0 = \sum_\sigma \int_{\mathbf{k},\omega} \bar{\chi}_\sigma(\mathbf{k},\omega)\left(-i\omega + \frac{1}{2m}(k_z^2 - k_f^2)\right)\chi_\sigma(\mathbf{k},\omega) + \sum_\sigma \int_{\mathbf{k},\omega} \bar{\psi}_\sigma(\mathbf{k},\omega)\left(-i\omega + \frac{1}{2m}(|\mathbf{k}|^2 - k_f^2)\right)\psi_\sigma(\mathbf{k},\omega), \tag{1}$$

where $\sigma = \uparrow, \downarrow$. k_f and m are, respectively, the Fermi momentum and fermion mass, which, we take to be identical for both bands. We further consider local density-density repulsion between the fermions, as given by

$$S_I = S_I^{1\mathrm{D}} + U\int_{\mathbf{r},\tau} \bar{\psi}_\uparrow\psi_\uparrow\bar{\psi}_\downarrow\psi_\downarrow + V\sum_{\sigma,\sigma'}\int_{\mathbf{r},\tau} \bar{\chi}_\sigma\chi_\sigma\bar{\psi}_{\sigma'}\psi_{\sigma'}. \tag{2}$$

Here, U sets the repulsion within the 3D band, V the repulsion between the two bands, and $S_I^{1\mathrm{D}}$ allows for a general form of interactions within the 1D band.

In this paper we study the effect of these interactions on the 3D fermions, and therefore trace out the 1D fermions (we discuss the feedback of the 3D fermions onto the 1D band in Appendix A). The leading effect comes from the effective interaction between 3D fermions as obtained by second order perturbation in V,

$$S_{\mathrm{eff}} = -\frac{V^2}{2}\sum_{\sigma,\sigma'}\int_{\mathbf{k}\mathbf{k}'\mathbf{q},\omega\omega'\Omega} \bar{\psi}_\sigma(\mathbf{k}+\mathbf{q},\omega+\Omega)\psi_\sigma(\mathbf{k},\omega) C(\mathbf{q},\Omega)\bar{\psi}_{\sigma'}(\mathbf{k}'-\mathbf{q},\omega'-\Omega)\psi_{\sigma'}(\mathbf{k}',\omega'). \tag{3}$$

$C(\mathbf{q},\Omega)$ is the Fourier transform of the density-density correlation function of the 1D band,

$$C(\mathbf{r},\tau) = \langle\bar{\chi}(\mathbf{r},\tau)\chi(\mathbf{r},\tau)\bar{\chi}(0,0)\chi(0,0)\rangle_{V=0} - \langle\bar{\chi}\chi\rangle^2_{V=0}. \tag{4}$$

In the absence of interactions, $S_I^1 = 0$, it is given by

$$C_0(\mathbf{q},\Omega) = \frac{Am}{2\pi q_z}\ln\frac{\Omega^2 + (2k_f q_z + q_z^2)^2/4m^2}{\Omega^2 + (2k_f q_z - q_z^2)^2/4m^2}, \tag{5}$$

where A is proportional to the Brillouin zone cross section, perpendicular to the k_z axis. $C_0(\mathbf{q},\Omega)$ has a logarithmic divergence for $q_z = \pm 2k_f$. When interactions within the 1D band are turned on, the χ fermions form a Luttinger liquid, with power law correlations. Had the 1D band been spinless, the $2k_f$ divergence would have had the form,

$$C(\mathbf{q},\Omega) \simeq \left[\Omega^2 + v^2(q_z \pm 2k_f)^2\right]^{K-1}, \tag{6}$$

where the effective Luttinger parameter K, as well as the velocity v associated with 1D charge fluctuations, are determined by the interaction terms in $S_I^{1\mathrm{D}}$. However, in the spinfull case there are two velocities, v_c and v_σ, for charge and spin excitations, respectively. Generally, $v_c \neq v_\sigma$, and the exact form of the correlation function is unknown, due to a lack of Lorentz invariance[12, 13]. Nevertheless, we shall assume $v_c = v_\sigma = v$ for simplicity. Qualitatively, our results depend only on the existence of enhanced $2k_f$ interactions, while their exact form is less important. Starting from the non-interacting case, $K = 1$, the parameter K is still expected to decrease for stronger repulsion within the 1D band. Thus, the sharpness of the interaction is tuned by the strength of these repulsive forces.

III. THE ELIASHBERG EQUATIONS

The main purpose of this paper is to study the superconducting phase which can emerge from the effective interaction, Eq. (3). To do so, one must solve the associated Eliashberg equations, since, this interaction depends strongly on frequency. The task is somewhat simplified if one approximates the interaction by its projection onto the Fermi surface, i.e., by mapping momenta $\mathbf{k}$ onto their polar angles θ, measured with respect to the positive k_z axis. Thus, the coupled *finite temperature* Eliashberg equations take the form

$$\Sigma(z,i\omega_n) = g\,T\sum_{i\omega_m}\int_{-1}^{1} dz'\,\lambda(z-z',\omega_n-\omega_m)\frac{\omega_m + \Sigma(z',i\omega_m)}{\sqrt{(\omega_m+\Sigma(z',i\omega_m))^2 + \Phi^2(z',i\omega_m)}} \tag{7}$$

$$\Phi(z,i\omega_n) = g\,T\sum_{i\omega_m}\int_{-1}^{1} dz'\,\lambda(z-z',\omega_n-\omega_m)\frac{\Phi(z',i\omega_m)}{\sqrt{(\omega_m+\Sigma(z',i\omega_m))^2 + \Phi^2(z',i\omega_m)}}. \tag{8}$$

$z = \cos\theta$ and $z' = \cos\theta'$ denote directions on the Fermi surface, T is the temperature, g is a unitless coupling constant and λ is the unitless interaction function. Note

that for density-density interactions such as we are considering here, the Eliashberg equations are identical for all singlet and triplet pairing channels. In the following we shall assume that λ takes the form

$$\lambda(z-z',\Omega) = \Big[\big((\Omega/\Lambda)^2+(z-z'-2)^2\big)^{K-1} - \big((\Omega/\Lambda)^2+(z-z'+2)^2\big)^{K-1}\Big] \frac{\Gamma(1-K)}{(z-z')\Gamma(K)} - \tilde{U}, \quad (9)$$

where $\Lambda = v_f k_f$ is a high energy cutoff, and $v_f = k_f/m$. This form does not contain the exact Luttinger Liquid correlation function, but it contains a $2k_f$ power-law divergence, which becomes logarithmic in the non-interacting case $K \to 1$, and is always positive. Furthermore, consistency with the $K \to 1$ limit sets $g = Ak_f^4 V^2/16\pi^2\Lambda^2$. The last term, with the unitless $\tilde{U} = Uk_f^3/4\pi\Lambda g$, comes from the local repulsion within the 3D band. By solving the Eliashberg equations, Eqns. (7,8), one obtains the self energy $\Sigma(z, i\omega_n)$ and pairing field $\Phi(z, i\omega_n)$, which we assume to be invariant under rotations about the k_z axis, as a function of the temperature T, the effective Luttinger parameter K, and the coupling constants, g and $\tilde{U}$.

We begin by considering the self energy $\Sigma(z, i\omega_n)$ in the absence of pairing. Setting $\Phi(z, i\omega_n) = 0$, and taking the zero temperature limit, eq. (7) becomes

$$\Sigma(z,\omega) = g\int_{\omega'}\int_{-1}^{1} dz'\lambda(z-z',\omega-\omega')\,\mathrm{sign}(\omega'). \quad (10)$$

In order to determine whether one finds a diverging self energy in this model, it is convenient to calculate its derivative. The most diverging term takes the form $\partial\Sigma/\partial\omega|_{\omega=0} \sim (1\pm z)^{2K-1}$, which indicates a diverging self energy at $z = \pm 1$ for $K \le 1/2$ (at $K = 1/2$ the divergence is logarithmic). Evaluating $\Sigma(z,\omega)$ itself at these points we find

$$\Sigma(z=\pm 1,\omega) \simeq -\frac{2\,g\,\omega}{2K-1}\left(2^{2K-1} - \frac{1}{2K}\left|\frac{\omega}{\Lambda}\right|^{2K-1}\right). \quad (11)$$

Consequently, we find that the renormalized quasiparticle weight, $Z(z,\omega) = (1-\partial\Sigma(z,\omega)/\partial\omega)^{-1}$, vanishes at the "north and south poles" of the Fermi surface, which are connected by the divergent $2k_f$ interaction. However, as far as pairing is concerned, the main effect of the non-Fermi-liquid behavior of these "hot spots", is to reduce the critical temperature, since, as we show later, these points are gapped in the superconducting phase.

Next, we address the Eliashberg equations in the superconducting phase. It turns out that it is not possible to obtain a triplet pairing solution, which requires $\Phi(-z, i\omega_n) = -\Phi(z, i\omega_n)$. To see this, we set $z = 1$ in the RHS of Eq. (8), and note that the main contribution to the LHS comes from the vicinity of $z = -1$. At these points the two sides of the equation have the opposite sign, which demonstrates that there is no triplet solution. Physically, this can be traced back to the real space oscillations of the correlation function, $C(\mathbf{r}, \tau)$, with period $2k_f$. Whereas the on site effective interaction between opposite spin particles, generated by these fluctuations, is attractive, it is negative at a distance πk_f^{-1}, which is the average distance between neighboring particles of identical spin. Thus, only singlet pairing is expected to emerge from this effective interaction. We note, however, that triplet pairing may arise from multi-orbital interactions when the orbital content varies as one goes around the Fermi surface.[14, 15]

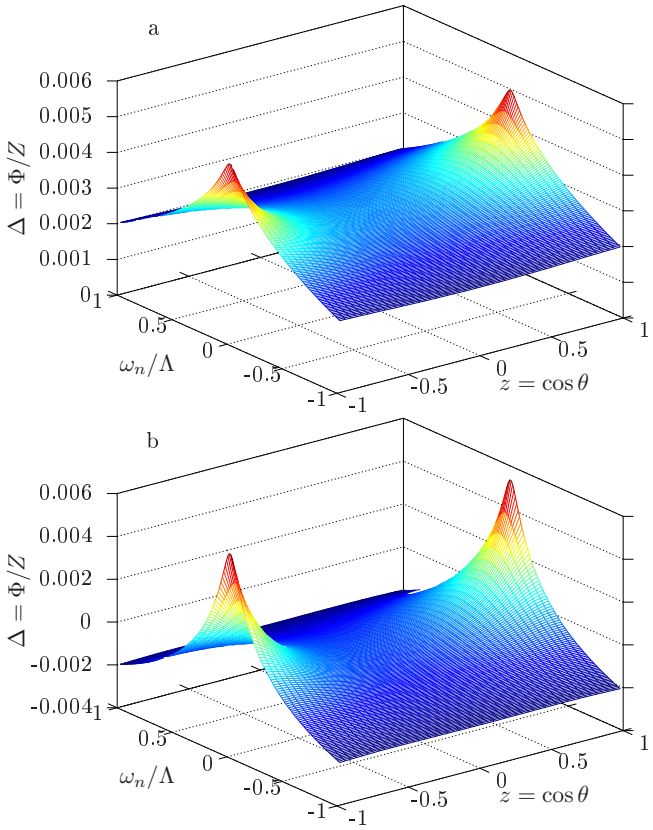

FIG. 2. Two examples of $\Delta(z, i\omega_n)$ as obtained by numerically solving the Eliasberg equations, Eqns. (7,8), for $K = 0.5$ and $T = 2\times 10^{-4}\Lambda$. (a) $\tilde{U} = 0$, $g = 0.422$. (b) $\tilde{U} = 1$, $g = 3.55$.

Finally, focusing on singlet pairing solutions, we used an iterative approach to solve for $\Sigma(z, i\omega_n)$ and $\Phi(z, i\omega_n)$ at finite temperature. To do this we restricted the Matsubara sum to run only over frequencies below a fixed high energy cutoff, $-\Lambda < \omega_n < \Lambda$, and divided the z-axis into small segments δz. Typically, we took $\delta z = 0.04$.

As discussed in the introduction, the divergent effective interaction results in gap functions, $\Delta(z, i\omega_n) = \Phi(z, i\omega_n)/Z(z, i\omega_n)$ which depend strongly on the Fermi surface position $z = \cos\theta$, and unconventional superconducting phases may emerge. Generally, Δ is peaked near the poles, $z = \pm 1$, and decreases as $z \to 0$, or with in-

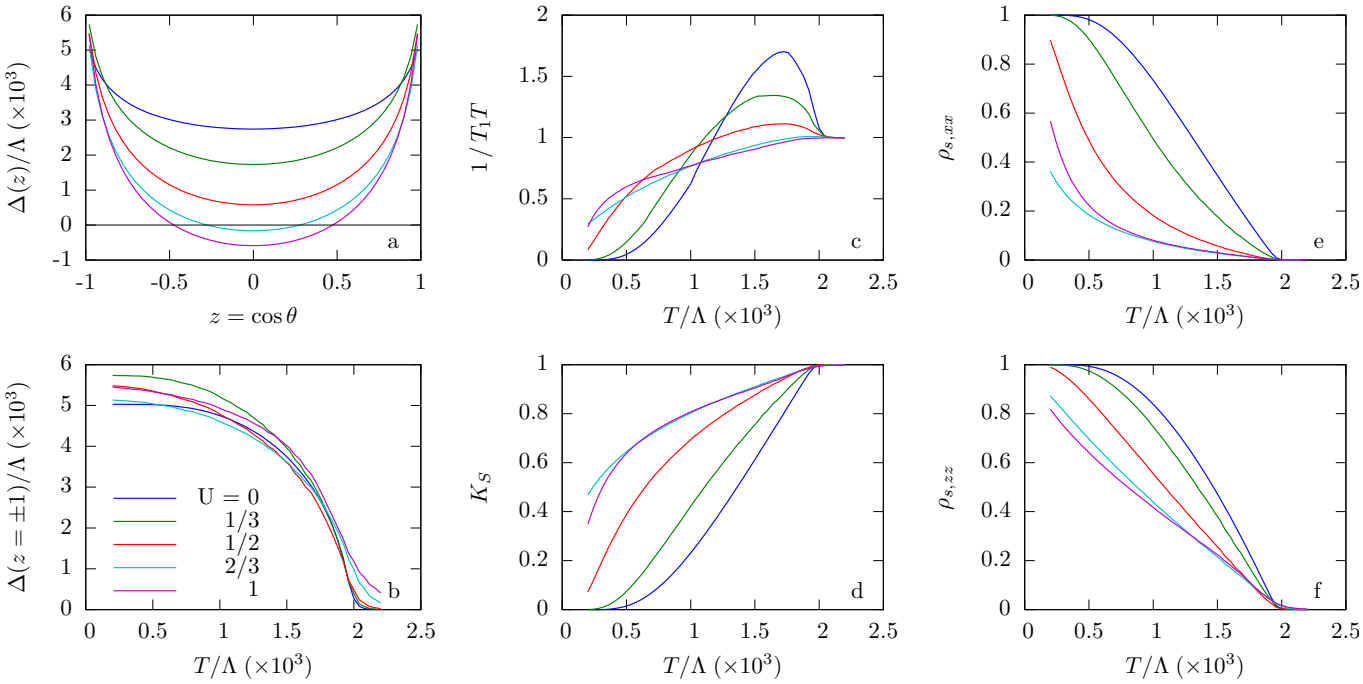

FIG. 3. (a) Low T gap function $\Delta(z)$. Nodal lines begin to appear for $\tilde{U} \gtrsim 0.6$. (b) $\Delta(z=\pm1)$ as a function of temperature. g was chosen such that for all choices of $\tilde{U}$, $T_c \simeq 0.002\Lambda$. (c) Nuclear spin relaxation rate, $1/T_1T$, normalized to its value at T_c. (d) Knight Shift, K_S, normalized to its value at T_c. (e)-(f) Superfluid stiffness in the x and z directions, normalized to their value at $T = 0$.

creasing ω. Under some conditions, the pairing function exhibits nodal lines, defined as the collection of points on the Fermi surface where $\lim_{\omega\to 0}\Delta(z,\omega) = 0$. These occur when the local repulsion $\tilde{U}$ is strong enough to suppress the uniform pairing, s-wave-like solutions, and favours d_{z^2}-wave-like solutions, with a pair of nodal rings at $\pm z_0$. Two example solutions are shown in Figure 2.

IV. EXPERIMENTAL CONSEQUENCES

Unconventional pairing is often manifested in various experimentally observable quantities. In the following, we show how increasing the local repulsion $\tilde{U}$ introduces nodal lines into the gap function Δ, which in turn dramatically effect several observables. Specifically, we use the zero frequency limit, $\Delta(z) \equiv \lim_{\omega\to 0}\Delta(z,\omega)$, as obtained from our numerical solutions of Eqns. (7,8), to approximately calculate the real time spin correlation fucntion $\chi_0(\mathbf{q},\omega)$ from which we obtain[16] the Knight shift, $K_S \sim \lim_{\mathbf{q}\to 0}\chi_0(\mathbf{q},0)$, and spin relaxation time T_1, as given by

$$\frac{1}{T_1T} \sim \int_{\mathbf{q}} \frac{\mathrm{Im}\chi_0(\mathbf{q},\omega)}{\omega}. \tag{12}$$

In addition we calculate the superfluid stiffness[17] tensor components, ρ_{xx} and ρ_{zz}, which are related to London penetration depth and μSR measurements. See Appendix B for details. In figure 3 we show results for several systems with $K = 1/2$ and varying $\tilde{U} = 0, 1/3, 1/2, 2/3, 1$. For each $\tilde{U}$ we chose, respectively, $g = 0.422, 0.885, 1.52, 2.4, 3.55$ such that the critical temperature T_c remained approximately the same, i.e., $T_c \approx 0.002\Lambda$, see fig. 3b. Fig. 3a depicts the low temperature gap function $\Delta(z)$, which exhibits nodal lines for $\tilde{U} \gtrsim 0.6$. When the repulsion in the 1D band is stronger, K decreases and the nodes appear for lower values of $\tilde{U}$. These nodes first appear at the "equator", $z = 0$, and move outward towards the "poles" as $\tilde{U}$ is increased. Figure 3c shows $1/T_1T$ as a function of temperature. Fully gapped Fermi surfaces exhibit a Hebel-Slichter peak below T_c, due to constructive contribution of quasiparticles to the spin relaxation process, as given by the BCS coherence factors. In our model, the height of the peak decreases together with the gap minimum, until it vanishes when the nodal lines are formed at high enough $\tilde{U}$. In conventional superconductors there is a drop in the Knight shift below T_c. As evident from figure 3d, this drop becomes less steep for larger $\tilde{U}$. Finally, ρ_{xx} and ρ_{zz} decrease linearly with T at low temperatures when the gap function has nodes, while they remain roughly constant at low T when the system is fully gapped. The striking difference bwtween the T dependence of ρ_{xx} and ρ_{zz}, as seen in figures 3e,f, is due to the large anisotropy in the gap function, as one moves on the Fermi surface from the "poles", $z = \pm1$, to the "equator", $z = 0$. Furthermore, a quasiclassical treatment[18], as well as general scaling considerations[19], indicate that, in the pres-

ence of nodal lines, the magnetic field dependence of the specific heat is expected to follow $\sqrt{H}$. This is attributed to the linear dependence of the quasiparticle density of states on energy.

V. DISCUSSION

The model considered in this paper, given by Eqns. (1) and (2), is a caricature of the more realistic models studied previously in the context of the new Cr based superconductors [8, 9, 14, 15]. It is therefore important to consider under what conditions our results hold, when the model is made more realistic. In our band structure, Eq. (1), there are two idealized features, namely, the of transverse dispersion in the 1D band, and the identical k_f for both 1D and 3D bands. The former ensures the presence of divergent fluctuations together with the absence of long range order, while the latter enables the efficient coupling of the 3D band to the divergent fluctuations. Relaxing these approximations cuts-off the $2k_f$ divergence in Eq. (3), making the effective interaction more modestly peaked. Qualitatively, this is not expected to change the superconducting phase, besides reducing T_c and increasing the values of $\tilde{U}$ required to obtain a nodal ring in the gap function. Other details, such as deviations from a spherical Fermi surface and differences between the 3D Fermi and 1D Luttinger velocities, are also not expected to alter the qualitative picture. Ultimately, however, the addition of weak transverse dispersion in the 1D band, will make it susceptible to pairing at low enough temperatures, possibly independent of the pairing in the 3D band.

In the main text we have considered only the effect of density-density interactions between bands, Eq. (2), which, as discussed in Appendix A, are consistent with the assumption of Luttinger liquid correlations for the 1D electrons. Such terms are generic, and exist in any electronic system. On the other hand, additional interaction terms may exist, and if dominant enough may change the nature of the superconducting phase. Specifically, pair hopping terms are expected, in general, when the bands have a non trivial orbital content, or, due to a finite Hund's rule coupling between bands. These interaction terms would induce pairing in the 1D band by established pairing in the 3D band. Furthermore, similar conditions may give rise to triplet superconductivity, as obtained in Refs. [14, 15]. Nevertheless, our results are expected to hold when these additional terms are weak, and could be neglected.

In summary, we have studied the superconducting phase expected to arise from $2k_f$ density fluctuations in a model of interacting 1D and 3D electrons. By solving the Eliashberg equations we have shown that strongly anisotropic singlet pairing forms on the 3D Fermi sphere. Nodal rings are formed in the gap functions when strong enough local repulsion is included. We have further shown that our simple model is sufficient to reproduce some of the striking experimental measurements in the Cr based superconductors, associated with the existence of nodal rings in the gap function.

ACKNOWLEDGMENTS

We are grateful to Sung-Sik Lee for useful discussion. This work was supported by the NSERC of Canada, the Canadian Institute for Advanced Research, and the Center for Quantum Materials at the University of Toronto.

Appendix A: Feedback of 3D fluctuations on 1D band

Coupling between 1D and 3D bands affects not only the electrons in the 3D band but also those in the 1D band. It is simpler to study this effect by visualizing the 1D band as a two-dimensional array of disconnected chains,

$$S_0 = \sum_{i\sigma} \int_{k,\omega} \bar{\chi}_{i\sigma}(k,\omega) \left(-i\omega + \frac{1}{2m}(k^2 - k_f^2) \right) \chi_{i\sigma}(k,\omega), \tag{A1}$$

where i enumerates the chains. The effective density-density interaction obtained by integrating out the 3D fermions, to second order in V, is given by

$$S^1_{\text{eff}} \sim -\frac{V^2}{2} \sum_{ij\sigma\sigma'} \int_{kk'q,\omega\omega'\Omega} \bar{\chi}_{i\sigma}(k+q,\omega+\Omega)\chi_{i\sigma}(k,\omega) \Pi_{ij}(q,\Omega)\bar{\chi}_{j\sigma'}(k'-q,\omega-\Omega)\chi_{j\sigma'}(k',\omega'). \tag{A2}$$

Here, $\Pi_{ij}(q,\Omega)$ is defined as

$$\Pi_{ij}(q,\Omega) \equiv \int dr d\tau \, \Pi(\mathbf{r}_i - \mathbf{r}_j + r\hat{\mathbf{z}}, \tau) e^{iqr - i\Omega\tau}, \tag{A3}$$

where $\Pi(\mathbf{r},\tau)$ is the density-density correlation function of the 3D fermions, and $\mathbf{r}_i, \mathbf{r}_j$ are the two-dimensional coordinates of chains i and j. Within a chain, $i = j$, this effective interaction modifies the bare forward ($q \simeq 0$) and back($q \simeq 2k_f$)- scattering interaction terms. Nevertheless, $\Pi_{ii}(q,\omega)$ is non-divergent and the 1D correlation functions are still expected to exhibit the power-law form of Eq. (6). On the other hand, the induced density-density interaction between chains, $-V^2\Pi_{ij}(q,\Omega)$, $i \neq j$, may, in principle lead to a charge-density ordered state. In this study, however, we assume that such tendencies are suppressed, for example, by long-range repulsion terms which we have not included explicitly in the model. Thus, for our purposes it is reasonable to neglect the induced coupling between chains.

We finally address the effect of 3D fluctuations on the dispersion of the 1D electrons. Referring again to the disconnected chains picture, we note that since the 1D Green's function obeys $\langle \bar{\psi}^1_i \psi^1_j \rangle \sim \delta_{ij}$, then also the self

energy must obey $\Sigma^1_{ij} \sim \delta_{ij}$. To see this it is sufficient to observe that all the diagrams in Σ^1 of any order contain only a single open fermion line, connecting the incoming and outgoing fermions. Consequently, the effective interaction does not induce dispersion which remains solely along the k_z axis.

Appendix B: Extracting superfluid stiffness and spin correlation function from the Bogolubov-de-Gennes spectrum

The task of extracting measurable quantities from the solutions of the Eliashberg equations, Eqns. (7, 8), is simplified by approximating the frequency dependent gap function by its zero frequency limit, $\Delta(z) = \lim_{\omega\to 0}\Delta(z,\omega)$. Beglubov-de-Gennes quasiparticles are well defined under such an approximation, and it is straight forward to extract measurable quantities from their spectrum. Thus, the superfluid stiffness, normalized to its $T = 0$ value, is given by

$$\rho_{ii} \simeq 1 - \frac{3(2\pi)^3\Lambda}{k_f^5}\int_{\mathbf{k}} k_i^2 \frac{\partial f}{\partial E_{\mathbf{k}}}, \tag{B1}$$

while the spin susceptibility is

$$\chi_0(\mathbf{q},\omega)=\frac{1}{4}\sum_{a,b=\pm}\int_{\mathbf{k}} \frac{f(aE_{\mathbf{k}}) - f(bE_{\mathbf{k+q}})}{\omega - aE_{\mathbf{k}} + bE_{\mathbf{k+q}} + i0^+} \left\{\left(1 + a\frac{\epsilon_{\mathbf{k}}}{E_{\mathbf{k}}}\right)\left(1 + b\frac{\epsilon_{\mathbf{k+q}}}{E_{\mathbf{k+q}}}\right) + ab\frac{\Delta_{\mathbf{k}}\Delta_{\mathbf{k+q}}}{E_{\mathbf{k}}E_{\mathbf{k+q}}}\right\}. \tag{B2}$$

Here, $\Delta_{\mathbf{k}}$ is obtained from the solution of the Eliashberg equations, $\epsilon_{\mathbf{k}} = k^2/2m$, $E_{\mathbf{k}} = \sqrt{\epsilon^2_{\mathbf{k}} + \Delta^2_{\mathbf{k}}}$, and $f(E_{\mathbf{k}})$ is the Fermi function. Note the BCS coherence factors which enter χ_0 and which are responsible for the appearance of the Hebel-Slichter peak below T_c in fully gapped superconductors.

[1] Jin-Ke Bao, Ji-Yong Liu, Cong-Wei Ma, Zhi-Hao Meng, Zhang-Tu Tang, Yun-Lei Sun, Hui-Fei Zhai, Hao Jiang, Hua Bai, Chun-Mu Feng, Zhu-An Xu, and Guang-Han Cao, "Superconductivity in Quasi-One-Dimensional $K_2Cr_3As_3$ with Significant Electron Correlations," Phys. Rev. X **5**, 011013 (2015).

[2] Zhang-Tu Tang, Jin-Ke Bao, Yi Liu, Yun-Lei Sun, Abduweli Ablimit, Hui-Fei Zhai, Hao Jiang, Chun-Mu Feng, Zhu-An Xu, and Guang-Han Cao, "Unconventional superconductivity in quasi-one-dimensional $Rb_2Cr_3As_3$," Phys. Rev. B **91**, 020506 (2015).

[3] Zhang-Tu Tang, Jin-Ke Bao, Zhen Wang, Hua Bai, Hao Jiang, Yi Liu, Hui-Fei Zhai, Chun-Mu Feng, Zhu-An Xu, and Guang-Han Cao, "Superconductivity in quasi-one-dimensional $Cs_2Cr_3As_3$ with large interchain distance," Sci. China Mater. **58**, 16–20 (2015).

[4] Tai Kong, Sergey L. Bud'ko, and Paul C. Canfield, "Anisotropic H_{c2}, thermodynamic and transport measurements, and pressure dependence of T_c in $K_2Cr_3As_3$ single crystals," Phys. Rev. B **91**, 020507 (2015).

[5] H.Z. Zhi, T. Imai, F.L. Ning, Jin-Ke Bao, and Guang-Han Cao, "NMR investigation of the quasi-one-dimensional superconductor $K_2Cr_3As_3$," Phys. Rev. Lett. **114**, 147004 (2015).

[6] D. T. Adroja, A. Bhattacharyya, M. Telling, Yu. Feng, M. Smidman, B. Pan, J. Zhao, A. D. Hillier, F. L. Pratt, and A. M. Strydom, "Superconducting ground state of quasi-one-dimensional $K_2Cr_3As_3$ investigated using μSR measurements," Phys. Rev. B **92**, 134505 (2015).

[7] G. M. Pang, W. B. Jiang, J. K. Bao, Z. F. Weng, Y. F. Wang, L. Jiao, J. L. Zhang, G. H. Cao, and H. Q. Yuan, "Evidence for nodal superconductivity in quasi-one-dimensional $K_2Cr_3As_3$," Phys. Rev. B **91**, 220502 (2015).

[8] Wu Xian-Xin, Le Cong-Cong, Yuan Jing, Fan Heng, and Hu Jiang-Ping, "Magnetism in Quasi-One-Dimensional $A_2Cr_3As_3$ (A=K,Rb) Superconductors," Chinese Phys. Lett. **32**, 057401 (2015).

[9] Hao Jiang, Guanghan Cao, and Chao Cao, "Electronic structure of quasi-one-dimensional superconductor $K_2Cr_3As_3$ from first-principles calculations," Scientific Reports **5**, 16054 (2015).

[10] J. C. Armici, M. Decroux, Ø. Fischer, M. Potel, R. Chevrel, and M. Sergent, "A new pseudo-one-dimensional superconductor: $T\ell_2Mo_6Se_6$," Solid State Communications **33**, 607–611 (1980).

[11] D. Jérome and H. J. Schulz, "Organic conductors and superconductors," Advances in Physics **31**, 299–490 (1982).

[12] Dror Orgad, "Spectral functions for the tomonaga-luttinger and luther-emery liquids," Philosophical Magazine Part B **81**, 377–398 (2001).

[13] Aníbal Iucci, Gregory A. Fiete, and Thierry Giamarchi, "Fourier transform of the $2k_F$ Luttinger liquid density correlation function with different spin and charge velocities," Phys. Rev. B **75**, 205116 (2007).

[14] Xianxin Wu, Fan Yang, Congcong Le, Heng Fan, and Jiangping Hu, "Triplet p_z-wave pairing in quasi-one-dimensional $A_2Cr_3As_3$ superconductors (A = K, Rb, Cs)," Phys. Rev. B **92**, 104511 (2015).

[15] Yi Zhou, Chao Cao, and Fu-Chun Zhang, "Theory for superconductivity in alkali chromium arsenides $A_2Cr_3As_3$ (A= K, Rb, Cs)," arXiv preprint arXiv:1502.03928 (2015).

[16] N. Bulut and D. J. Scalapino, "Weak-coupling model of spin fluctuations in the superconducting state of the layered cuprates," Phys. Rev. B **45**, 2371–2384 (1992).

[17] Douglas J. Scalapino, Steven R. White, and Shoucheng Zhang, "Insulator, metal, or superconductor: The criteria," Phys. Rev. B **47**, 7995–8007 (1993).

[18] Volovik, G. E., "Superconductivity with lines of GAP nodes: density of states in the vortex," **58**, 469 (1993).

[19] Steven H. Simon and Patrick A. Lee, "Scaling of the Quasiparticle Spectrum for d-wave Superconductors," Phys. Rev. Lett. **78**, 1548–1551 (1997).